COMPLETION OF THE FIRST TF COIL STRUCTURE OF ITER

M. NAKAHIRA, M. IGUCHI, T. SAKURAI, H. OZEKI, E. FUJIWARA, K. TAKANO, Y.S. HONG, M. INO, M. NISHINO, N. KOIZUMI
National Institutes for Quantum and Radiological Science and Technology (QST)
Chiba-shi, Japan
Email: nakahira.masataka@qst.go.jp

N. SAWA, D. HARA, T. INAGAKI
Mitsubishi Heavy Industries, LTD
Kobe, Japan

S.Y. KIM, J.H. CHOI, S.S. HWANG
Hyundai Heavy Industries
Ulsan, Republic of Korea

C. LUONGO
ITER Organizaation (IO)
St. Paul-lez-Durance Cedex, France

Abstract

The first ITER Toroidal Field Coil Structures (TFCS) has been successfully completed by Japan Domestic Agency (JADA) in Japan and Korea. There were 5 major challenges for the TFCS fabrication. This paper describes these challenges and solution established during fabrication and how to implement to the ITER TFCS.

1. INTRODUCTION

This paper reports the completion of the first of nineteen ITER Toroidal Field Coil Structures (TFCSs), the procurement responsibility of which is 100% that of the Japan Domestic Agency (JADA). The major technical challenges of the TFCSs of ITER are (i) development of new materials having high ductility under cryogenic temperatures (4 K), (ii) application of partial penetration welding (PPW), (iii) welding deformation control, (iv) development of specialized ultrasonic testing (UT) that factors in attenuation from austenitic stainless-steel weldments and (v) fitting the large (16 m × 9 m) complex D-shaped structure for closure welding (CW) within tolerances of 0.5 mm. Only by developing solutions for the respective challenges was the first ITER TFCS successfully completed.

The ITER TFCSs are massive 16 m × 9 m welded structures made of austenitic stainless steel that encase the superconducting TF coils winding pack (WP) with a final closure weld, which requires extremely precise dimension-controlled structures to fit the closure weld root. The TFCSs must also support the weight and electromagnetic forces of the TF coils and be highly ductile at cryogenic temperatures of 4 K to retain structural integrity during superconducting operation. A TFCC consists of 4 sub-assemblies (AU, AP, BU and BP) as shown in Fig. 1.

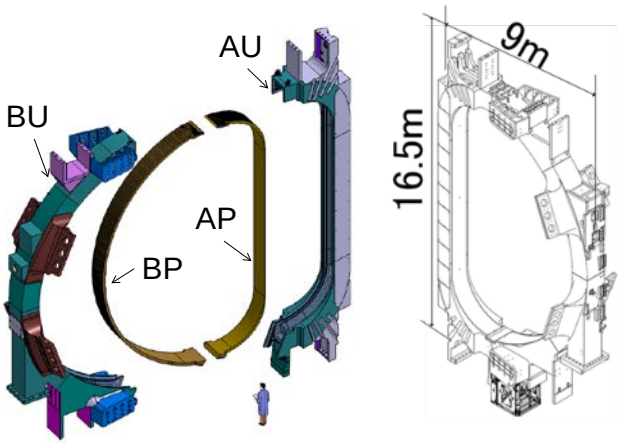

FIG. 1. ITER TF Coil Structure

The views and opinions expressed herein do not necessarily reflect those of the ITER Organization.

2. FABRICATION OF ITER TFCS

2.1. Challenge (i): Material development

JADA has developed cryogenic structural material for the fusion experimental reactor for 30 years [1]. ITER superconducting coil have to ensure huge magnetic force in cryogenic environment. High stress is generated in the inner leg of TFC Structure and the maximum static stress intensity is about 667 MPa [2]. To maintain high ductility at cryogenic temperatures, a special austenitic stainless steel having more than 1000 MPa of yield strength and more than 200 MPam0.5 of fracture toughness (KIC) at a temperature of 4 K was developed (JJ1 (C1)) [3]. JADA figured out correlation between yield strength at 4K and C+N contents from the large amount of experimental data. [4] It can control yield strength by designing the C+N contents. Applying this knowledge, JADA also prepare 3 grades (C2:900, C3:700, C4:500MPa yield strength at 4K) of standard high-strength austenitic stainless steel 316LN. They are used depending on the required strength. JADA has a responsibility procure such a special material about 5000 ton with keeping high quality. In beginning of 2018, material procurement for TFCS was completed.

Generally, prospection of the fracture toughness by high accuracy was not enough developed. With such background, JADA has secured the specification of fracture toughness by 1) Using only qualified supplier, 2) Check by Charpy impact test, 3) Sampling inspection. To improve control parameter for fracture toughness, JADA performed surface observation after testing test piece and investigate large amount of sampling inspection date and additional trial, JADA discovering the strong correlation between Md30 and fracture toughness at 4K of material for ITER TFCS. (Fig.2) [5] Md30 is defined as the temperature which 50% martensitic transformation occurs when 0.3 strain is applied [6]. Originally, it's tendency of martensitic transformation. And it can be calculated by chemical composition and grain size. [7] As a validation, JADA confirmed high fracture material can be manufactured by control the Md30. [5] The Md30 value has been implemented as the scale of the sampling in the material procurement, which has improved the standard of quality.

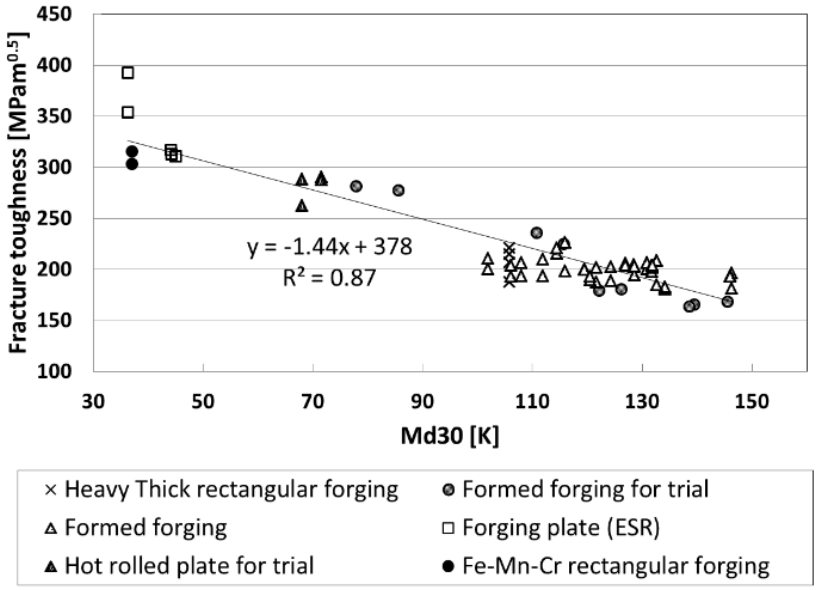

FIG.2 Correlation between the fracture toughness and Md_{30}

2.2. Challenge (ii): Partial Penetration Welding

The TFCSs have support attachments of PF and correction coils some of which require partial penetrate welding (PPW) or fillet welding (FW). The PPW and FW joints have unwelded area at back side of weld root which is regarded as as-weld notch having high stress concentration. During ITER operation, this as-weld notch takes static and cyclic load at cryogenic temperature. However, since there was no specific design procedure for PPW and FW joints at cryogenic temperature, design assessment process and non-destructive examination (NDE) method had to be established to verify structural integrity.

At first, fatigue crack growth (FCG) behaviour and properties was confirmed [8]. The compact tension (CT) specimens were prepared from a mock-up of actual joint shape of PPW, double J-groove (Fig. 3-a)). The specimens are the one having as-weld notch (Fig. 3-b) and those having electronic discharge machining (EDM)

notch with 0.2mm diameter at tip, which configuration are shown in Fig. 3-c), -c-1) and -c-2). FCG ratio (FCGR) tests were carried out under load control condition with stress ratio of 0.1 and target initial ΔK of 28 MPam$^{0.5}$. From test results, it was decided to apply fracture mechanics assessment to design process, because crack in CT specimen having as-weld notch grew from just after start of FCGR test but one having EDM notch needed longer cycle to start crack growth. In addition, it could be said; 1) since crack in all CT specimen grew in weld metal, crack propagation analysis in weld metal was enough (Fig. 4-a), and 2) properties of Paris's law obtained from these FCGR test was able to apply for FCG analysis (Fig. 4-b).

Design by analysis was carried out by finite element (FE) models covering total 133 weld joints applying above FCGR test results. As the results of FE analyses, allowable initial defect sizes were defined for each weld joint to keep structural integrity during ITER operation. The minimum defect size to be detected in PPW/FW is 100mm^2 of semi-elliptical at the root of the partial penetration weld, with an initial aspect ratio of 3 (4.6mm of minor radius, 13.8mm of major radius).

Because of accessibility and workability, Ultrasonic Testing (UT) method is applied as NDE for PPW joints. In order to confirm detectability of UT in PPW joint, verification test of UT by using mock-up having PPW joint was carried out. From this verification test result, it was shown that conventional UT method according to ISO standards can measure welding depth with +/- 1mm accuracy. Based on this result, UT procedure for PPW was defined that measure the PPW joint depth, compare the design depth, calculate difference from design, and compare acceptable size for the depth, and length obtained by scanning distance. For FW, progressive die penetrant test (PPT) is applied as alternative NDE method of UT, which PT is applied to first welding layer and to each three welding layers.

In order to establish the design assessment process for PPW in cryogenic temperature, FCG behaviour and properties of actual material with as-weld notch had to be confirmed. In addition, NDE method for PPW and FW joints to detect minimum allowable defect had to be developed. To solve them, JADA clarified the FCG behaviour of PPW under cryogenic temperature using CT specimen prepared from mock-up having actual PPW joint, and established NDE method by verifying detectability of PPW joint. These activities have been completed successfully. According to these establishments, JADA has completed design assessment for all PPW and FW joints.

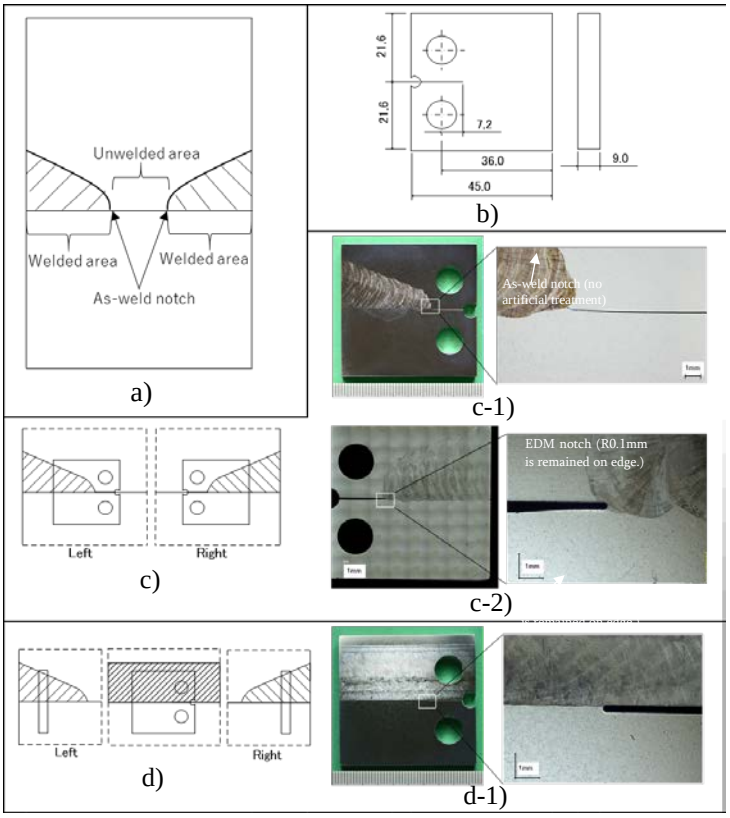

FIG.3 Information for mock-up and CT specimens, a) illustration of mock-up having actual PPW joint shape, b) dimension of CT specimen, c) sampling position of CT specimens for as-weld and EDM notch(EDM dia.0.2mm applied to as-weld notch and finally R0.1mm is remained on edge) , c-1) photograph of CT specimen having as-weld notch, c-2) photograph of CT specimen replaced as-weld notch with EDM notch, d) sampling position of CT specimens for weld metal, d-1) photograph of CT specimen for weld metal

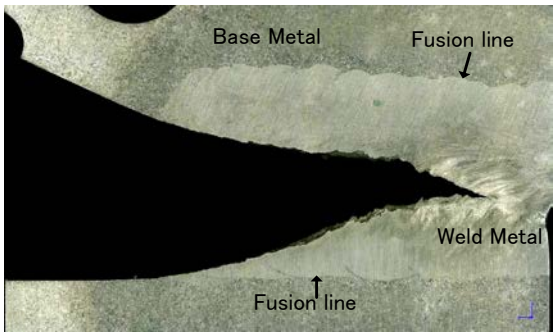

a)

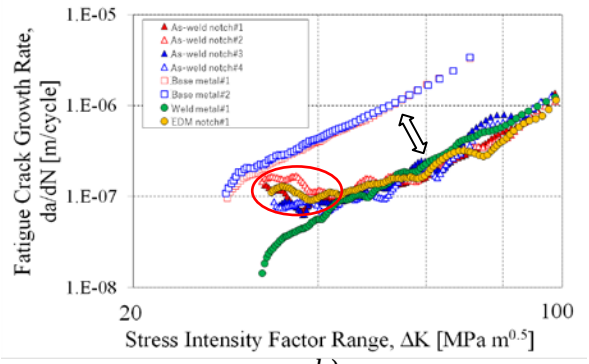

b)

FIG.4 FCGR test result, a) Photograph overview of as-weld notch type after FCG test with etching by aqua regia, b) FCGR test results for all specimens

2.3. Challenge (iii): Welding Deformation Control

Particular attention must be given to the welds of the TFCS to confirm structural integrity at cryogenic temperatures and to control welding deformations. JADA performed welding qualification using mock-ups. Test pieces were sampled from these mock-ups, and mechanical properties, such as fracture toughness and yield strength, were checked at cryogenic temperatures [9-11]. Mechanical properties of welding joints also satisfy ITER requirement (YS>500, 700, 900 and1000 MPa, K_{IC}>180 MPa·$m^{0.5}$).
TFCS consists of 4 Subassemblies (SAs) which are called AU, BU, AP and BP. Because SAs are too huge, JADA manufactures them in units of Basis Segment (BS) and weld Segment-to-Segment. U-shape is formed from welding 1 outer plate and 2 side plates. Welding deformation was controlled by using a special welding process to compensate for angular distortion [9, 11-12]. Segment-to-segment welding proved the most difficult because unlike flat plate welding, the complex U-shape makes angular distortion difficult to estimate. JADA performed segment-to-segment (A1+A2) welding trial, and amount of welding deformation and tendency of welding direction are figured out. [13-14] Figure 5 shows an example of the segment-to-segment welding configuration using controlled deformation. A1 is initially offset from the result of trial and deforms towards the reference line.

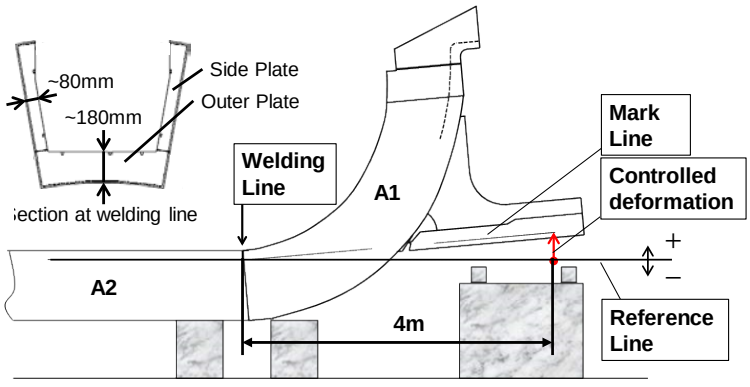

FIG. 5. Segment-to-segment welding (A1-A2)

Figure 6 shows a controlled deformation for the first actual AU with respect to the total deposit of the weld. The initial offset was approximately 4 mm and the gap from the reference line was controlled to be within a +2 mm margin, as deformation beyond the reference line was prohibited.

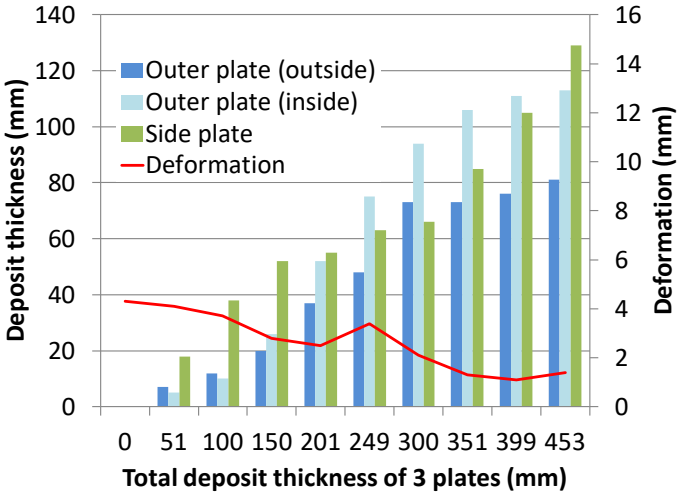

FIG. 6. Example of welding deformation

2.4. Challenge (iv): Ultrasonic Test

Since the coil case is a large-sized welded structure, the reliability of the volumetric examination that guarantees the welding quality is important for securing structural integrity.
At where a radiographic examination is difficult from the size of the coil case, ultrasonic examination is used. The longitudinal wave is selected which is generally used for austenitic stainless-steel welds. There is concern that the signal level will decrease due to attenuation, because the ultrasonic wave propagates through the weld metal of austenitic stainless steel over a long distance. The attenuation of the UT beam in the weld is compensated for by the transfer correction factor obtained from welding a test piece made of the actual TFCS material and weld metal during calibration.
Figure 7 shows the concept of weld attenuation calibration. Ultrasonic examination is performed using Distance amplitude characteristic (DAC) curve obtained by base material calibration block considering the sensitivity difference of signal level obtained by the reference block made of actual TFCS material and weld metal. For this, the relationship between sensitivity difference vs propagation distance in weld metal was obtained.
Figure 8 shows test results obtained by manufacturing companies. It was confirmed that the sensitivity difference (y) has a positive linear correlation as “y =ax” with the propagation distance(x) in the weld metal.

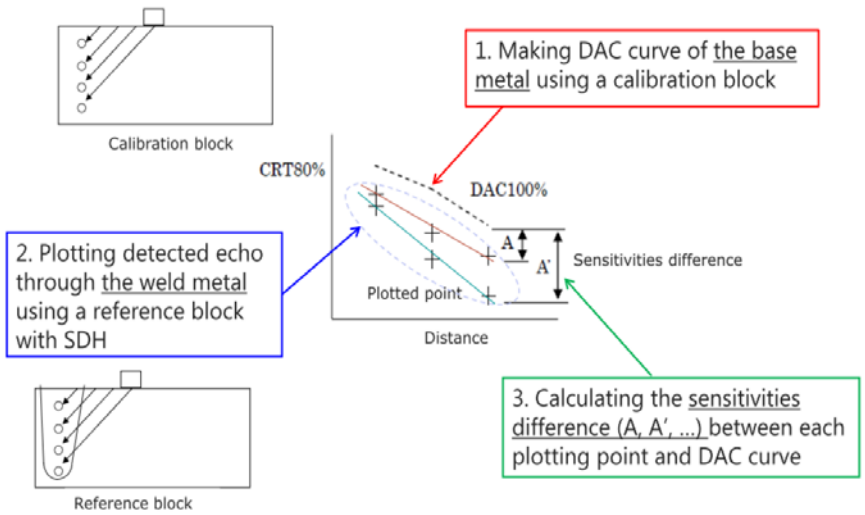

FIG. 7. Concept of sensitivity setting for attenuation by weld metal

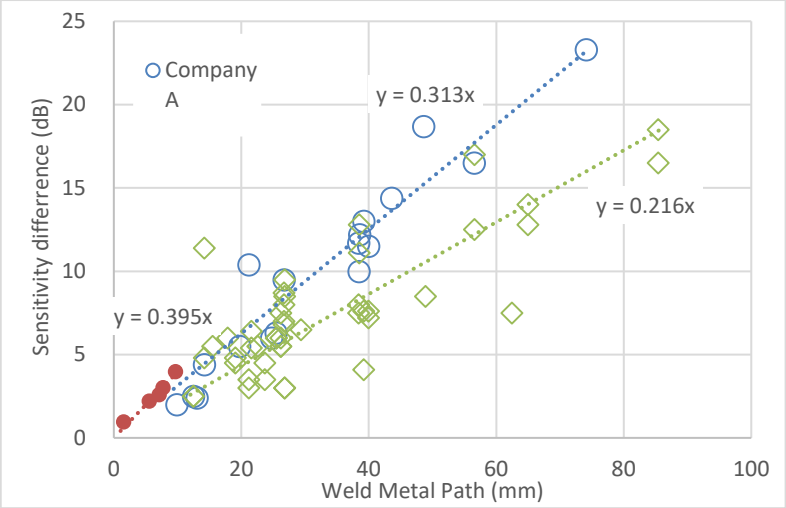

FIG. 8. Sensitivity difference by propagation distance through weld metal

2.5. Challenge (v): Fitting Test

The final machining of the TFCS was performed along its closure welding root having a gap and misalignment tolerance between two welding edges of around 0.5 mm, which required precise temperature control/compensation. Figure 9 shows tolerances of the closure welding root matching. The tolerance for the root gap is 0.5 +/- 0.25 mm. For the misalignment, the tolerance is +/- 0.7 mm for the bottom plates of the U-shape, and +/- 0.3 mm for its side plates. The final machining of the weld root on the sub-assemblies were performed by 3 different companies using several different machines under temperature control environment within 20+/-5 degree Celsius as a target, or applying detail temperature correction factor obtained on the machine to perform final machining to avoid their mismatch due to the thermal expansion. In addition, custom machining was applied to the weld root on BU reflecting the actual AU bevel position measurement data. As a key activity to ensure the structural integrity, fitting tests of weld roots with actual AU and AP, BU and BP, and AU and BU were performed after the final machining and the following dimensional survey.

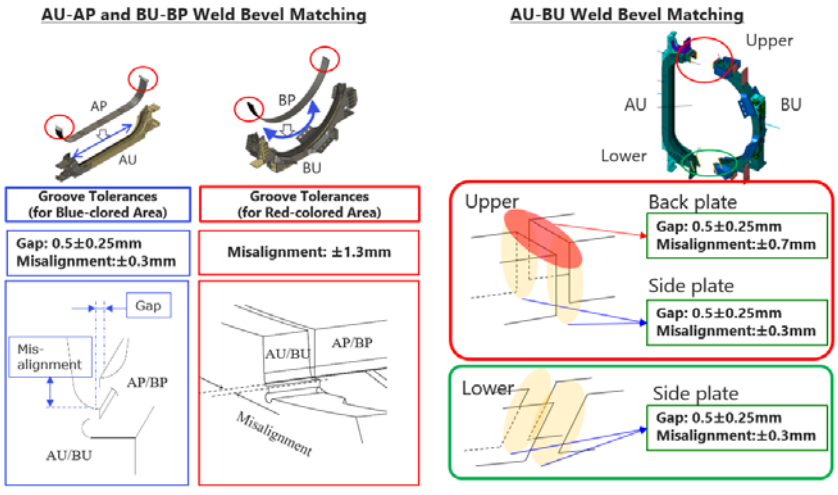

FIG. 9. Weld root matching tolerances of TFCS

Two types of the fitting test method are performed, one is for AU and AP test as shown in Fig. 10 and for BU and BP test. The other is for AU and BU test as shown in Fig. 11. In the former case, AU or BU was fixed on the ground to allow AP or BP to access slowly from the upper side. The difficulty is to control not only the precise position of AP and BP but also the flexibility of them which causes shape change during operation. Several types of guide jigs for AP and BP shown in Fig. 10 to adjust them to AU and BU welding root. Eventually the both tests were successfully completed.

In the case of AU and BU fitting test, both of them were laid down on the ground for EU01. Here, BU was fixed on the floor while AU was set on the rail guide. Then, AU was slid toward BU to match the root surface of the weld grooves. On the other hand, AU was set on the floor and BU was lifted down toward AU for JA01. In this case, BU position was adjusted using jacks with respect to jigs attached on AU.

The difficulty of this test was to find the exact position of AU and BU to achieve the target criteria. Thus, before the actual work of fitting-up, virtual fitting based on the dimension survey data of AU and BU was performed. The result of the virtual fitting successfully provided the position of AU and BU satisfying the target criteria of the welding root fitting. The actual fitting test was performed with monitoring the actual relative AU position to BU by laser tracker. In the result of fitting test, it was found that most of the weld root was fit within the tolerances of the gap and misalignment. The rest of the part was slightly out of the tolerance. However, it was judged that still welding could be applicable since the deviation was enough small. Finally, the manufacturing of all AU, AP, BU, and BP of the first product set was completed.

FIG. 10. AU-AP Fitting Test (Left) and guide jigs to control the position of AP (Right)

(a) EU01 Fitting test (b) JA01 Fitting test

FIG. 11. First completion of AU and BU Fitting Test

3. CONCLUSION

The first TFCS was arrived to the EU in March 2018 and the second TFCS also was arrived in July 2018 for assembly with the EU-manufactured WP to complete a TF Coil of ITER. The first TFCS for a Japan-manufacturing TF coil was completed its fitting test successfully in August 2018, acceptance test of its WP was completed in August 2018 and then the WP is cold-tested, and assembly of the TFCC and WP will be started from the fourth quarter of 2018 as the very first TF Coil of ITER.

ACKNOWLEDGEMENTS

The authors would like to express their sincere gratitude to Drs. M. Sugimoto, T. Inoue and K. Okuno for their continuous suggestions and encouragement during these activities. The authors also would like to acknowledge contributions of the Toshiba Corporation Power Systems Company for development of the specialized UT technique.

REFERENCES

[1] M. IGUCHI et al. “Cryogenic Structural Materials of the ITER Toroidal Field Coil Structure”, Proc. of SMINS-4, IV-1 (2016).

[2] ITER ORGANIZATION, “Design Description Document”, ITER IDM Reference 2MVZNX., version 2.2. (2009).

[3] J. ISHIZAKA, R. MIURA, H. NAKAJIMA, S. SHIMAMOTO, “Strength and Toughness of 12Cr-12Ni-10Mn-5Mo Steel for Cryogenic Structural Application”, Tetsu-to-Hagane, 76, (in Japanese) (1990) 149-156.

[4] H. NAKAJIMA, et al., “qualification of cryogenic structural materials for the iter toroidal field coils”, Proceedings of the ASME 2009 Pressure Vessels and Piping Division Conference, PVP2009- 77553, (2009)1-8.

[5] T. SAKURAI et al., “Correlation between the fracture toughness of the austenite stainless steel and martensitic transformation in cryogenic”, J. Cryo. Super. Soc. Jpn, Vol.52, No.4 (2017) 260-267.

[6] T. ANGEL, “Formation of martensite in austenitic stainless steels,” J. Iron Steel Inst., 177 (1954) 165.

[7] K. NOHARA, Y. ONO AND N. OHASHI: “Composition and grain size dependencies of strain-induced martensitic transformation in metastable austenitic stainless steels,” Tetsu-to-Hagane, 63 (1977) 772-782.

[8] M. IGUCHI et al., “Welding joint design of ITER toroidal field coil structure under cryogenic environment”, Proc. of ICONE23, 1713 (2015).

[9] M. IGUCHI, et al., “Development of structures for ITER toroidal field coil in Japan”, IEEE Transactions on Applied Superconductivity 22 (3 (June)) 4203305 (2012).

[10] M. IGUCHI, et al., “Mechanical properties of full austenitic welding joint at cryogenic temperature for the ITER toroidal field coil structure”, Fus. Eng. Des. Vol. 88, Issues 9–10 (2013) 2520-2524.

[11] T. SAKURAI et al., “Mechanical Properties of Welded Joint at Cryogenic Temperature for Manufacturing of ITER TF Coil Structure”, IEEE Trans. Appl. Supercond., Vol.26, No.4, 4204705 (2016).

[12] M. IGUCHI, et al., “Progress of manufacturing trial for the ITER toroidal field coil structure”, Appl. Supercond. IEEE Trans. 24 (3) 3801004 (2013).

[13] M. IGUCHI, et al., Development of structures for the ITER Toroidal Field Coil in Japan, Appl. Supercond. IEEE Trans. 28 (3(Dec.)) 4202105 (2018).

[14] T. SAKURAI et al., “Development of manufacturing technology for ITER TF Coil Structure”, Fus. Eng. Des. 109 (2016) 1592-1597